# Ultraviolet Radiation Significantly Enhances the Molecular Response to Dispersant and Sweet Crude Oil Exposure in *Nematostella vectensis*

Ann M. Tarrant[a,#], Samantha L. Payton[b,#], Adam M. Reitzel[a,c], Danielle T. Porter[b,d], Matthew J. Jenny[b,*]

From the [a]Biology Department, Woods Hole Oceanographic Institution, Woods Hole, MA 02543, [b]Department of Biological Sciences, University of Alabama, Tuscaloosa, AL 35487, [c]Department of Biological Sciences, University of North Carolina at Charlotte, Charlotte, NC 28223, [d]Department of Neurobiology and Anatomical Sciences, University of Mississippi Medical Center, Jackson, MS 39216

[#]These authors contributed equally to this work.

*Address correspondence: Matthew J. Jenny, Department of Biological Sciences, Box 870344, University of Alabama, Tuscaloosa, AL 35487, USA. Tel: 205-348-8225, Fax: 205-348-1786, Email: mjjenny@ua.edu

Running title: *Nematostella* Response to Abiotic Stressors

**ABSTRACT**

Estuarine organisms are subjected to combinations of anthropogenic and natural stressors, which together can reduce an organisms' ability to respond to either stress or can potentiate or synergize the cellular impacts for individual stressors. *Nematostella vectensis* (starlet sea anemone) is a useful model for investigating novel and evolutionarily conserved cellular and molecular responses to environmental stress. Using RNA-seq, we assessed global changes in gene expression in *Nematostella* in response to dispersant and/or sweet crude oil exposure alone or combined with ultraviolet radiation (UV). A total of 110 transcripts were differentially expressed by dispersant and/or crude oil exposure, primarily dominated by the down-regulation of 74 unique transcripts in the dispersant treatment. In contrast, UV exposure alone or combined with dispersant and/or oil resulted in the differential expression of 1,133 transcripts, of which 436 were shared between all four treatment combinations. Most significant was the differential expression of 531 transcripts unique to one or more of the combined UV/chemical exposures. Main categories of genes affected by one or more of the treatments included enzymes involved in xenobiotic metabolism and transport, DNA repair enzymes, and general stress response genes conserved among vertebrates and invertebrates. However, the most interesting observation was the induction of several transcripts indicating *de novo* synthesis of mycosporine-like amino acids and other novel cellular antioxidants. Together, our data suggest that the toxicity of oil and/or dispersant and the complexity of the molecular response are significantly enhanced by UV exposure, which may co-occur for shallow water species like *Nematostella*.

**KEYWORDS**

hydrocarbons, UV radiation, biomarker, chemical pollution, environmental toxicology, RNA sequencing, cnidarian

## 1. INTRODUCTION

The Deepwater Horizon oil spill in April 2010, resulted in the release of an estimated 4.9 million barrels of sweet crude oil over a period of 87 days, and initial responses included the surface and subsurface application of approximately 1.8 million gallons of chemical dispersant (Ramseur, 2010). As a result, salt marsh organisms were exposed to weathered and dispersed sweet crude oil, and oil-derived compounds (Natter et al., 2012; Stout et al., 2016). This resulted in extensive mortality of saltmarsh plants, particularly in heavily oiled areas (Lin and Mendelssohn, 2012). Benthic invertebrates were impacted both through direct toxicity of the oil, and indirectly through loss of seagrass habitat, and trophic interactions. Observed effects on benthic invertebrates in oiled marsh areas included suppression of crab burrowing (McCall and Pennings, 2012), as well as reduced meiofaunal abundance and diversity (Fleeger et al., 2015), periwinkle abundance (Zengel et al., 2016), and shrimp growth rates (Rozas et al., 2014).

Major constituents of crude oil, a complex mixture of aromatic and non-aromatic hydrocarbons, include the polycyclic aromatic hydrocarbons (PAHs), a group of toxic compounds that pose a significant risk to humans and other animals. Exposure of animals to PAHs can result in oxidative stress and can compromise immune function, endocrine regulation and development (reviewed by Hylland 2006). Among animals, molecular responses to PAH exposure are best understood in vertebrates, where the aryl hydrocarbon receptor (AHR) pathway is the major regulatory pathway. In vertebrates, AHR is a ligand-activated, inducible transcription factor that pairs with its dimerization partner, AHR nuclear translocator (ARNT), to regulate the expression of a battery of phase I and phase II metabolic enzymes. The primary AHR target gene and classic biomarker of vertebrate hydrocarbon exposure is cytochrome P450 1A (CYP1A), a phase I oxidative enzyme that plays a major role in the biotransformation of aromatic hydrocarbons. The AHR pathway also regulates the expression of phase II enzymes that play a role in the conjugative biotransformation of hydrocarbons, such as glutathione S-transferases (GSTs) and UDP-glucuronosyltransferases (UDPGTs), which facilitate excretion and prevent reabsorption of the hydrocarbons. In addition to these AHR-mediated effects, studies in diverse animal groups have shown that PAH exposure leads to widespread physiological responses; among these, up-regulation of defenses against oxidative stress, including antioxidant genes, non-enzymatic antioxidants, and heat shock proteins is typically observed (e.g., Hannam et al., 2010, Jenny et al., 2016). This cellular response is largely driven by the nuclear factor (erythroid-derived 2)-like 2 (NRF2) transcription factor, often considered to be a master regulator of the oxidative stress response. Activation of this pathway is mainly driven by the potential for cytochrome P450 monooxygenases, e.g. CYP1A, to generate significant amounts of reactive oxygen species, which contributes to toxicity, as a result of inefficient metabolism of cytochrome P450 substrates (Schlezinger et al., 1999, 2006).

In cnidarians, PAH, oil and dispersant toxicity have primarily been studied in tropical reef-building corals, through studies motivated by concerns about potential impacts of oil exposure on reefs. Within natural coral populations, oil exposure has been shown to result in bleaching, tissue retraction, photoinhibition of symbionts, impaired reproduction, and increased occurrence of injuries; however the cellular pathways underlying these effects are poorly known (reviewed by van Dam et al., 2011). Experimental studies have shown that corals can rapidly take up environmentally relevant concentrations of PAHs and polychlorinated biphenyls (PCBs) (Solbakken et al., 1984; Kennedy et al., 1992), both strong activators of the AHR pathway in vertebrate model organisms. However, despite the potential for rapid uptake, corals often concentrate hydrophobic contaminants in their lipid-rich tissues and exhibit poor excretion (Denton et al., 2006; Peters et al., 1997). Some studies have demonstrated low ethoxyresorufin O-dealkylation (EROD) activity, a catalytic measurement of CYP1A activity, in cnidarian (sea anemone) tissues (Heffernan and Winston, 1998; Heffernan and Winston, 2000); while other studies have detected low activity of various phase I and phase II metabolic enzymes in corals, e.g., GST and UDPGT (Gassman and Kennedy, 1992). Thus, the concentration of hydrophobic contaminants in lipid-rich tissues of cnidarians is likely due in part to low rates of xenobiotic metabolism. While a few studies have attempted to characterize dose-response relationships and identify biomarkers of exposure (Rougée et al., 2006; Epstein et al., 2000; Negri and Heyward, 2000; DeLeo et al., 2016; Venn et al., 2009; Goodbody-Gringley et al., 2013), little is known regarding the molecular responses of cnidarians to oil or other petroleum-based pollutants. In addition, many of these studies have also quantified the toxicity of chemical dispersant and enhanced toxicity of dispersant-oil mixtures. Experimental exposure of corals to chemical dispersants alone has resulted in decreased settlement, metamorphosis and survival of coral larvae (Epstein et al. 2000; Negri and Heyward, 2000; Goodbody-Gringley et al., 2013); increased tissue mortality in corals and deepwater octocorals (DeLeo et al., 2016); and induction of a few stress-responsive genes in coral (Venn et al., 2009). Although these studies of dispersant exposure all found that co-exposure to oil and dispersants led to enhanced toxicity (increased severity of the previously mentioned effects) relative to either stressor alone, the associated molecular mechanisms are poorly known.

In addition to general toxicity from hydrocarbon and/or dispersant exposures, many marine invertebrates must also deal with the additional cellular stress that occurs from co-exposure to natural abiotic stressors, such as ultraviolet (UV) radiation. Furthermore, UV radiation can enhance PAH toxicity via through two primary mechanisms (reviewed by Neff, 2002). First, PAHs can absorb UV energy that can be transferred to molecular oxygen, resulting in the production of reactive oxygen species (ROS), such as singlet oxygen and superoxide radicals. The second mechanism results from photomodification of the parent PAH into secondary by-

products that can have similar or even greater toxicity. It should also be noted that the absorption of UV radiation by endogenous cellular compounds can result in the production of ROS. Finally, cellular DNA can directly absorb UVB radiation (290-320 nm) resulting in the formation of damaged photoproducts (reviewed in Pfeifer et al., 2005).

In a previous study, we exposed juveniles *Nematostella vectensis* (starlet sea anemone, *"Nematostella"* hereafter) to ultraviolet light and PAHs, both separately and in combination, and we observed greater mortality with the combination of stressors relative to either by itself. We also measured signification changes in transcription of some candidate biomarker genes associated with general cellular (heat shock proteins, HSPs) and oxidative stress (superoxide dismutases, SODs) (Tarrant et al., 2014). *Nematostella* is an estuarine denizen found along the eastern Atlantic seaboard of the United States and Canada (Reitzel et al., 2008). This species primarily inhabits sediments in shallow habitats with little flow where individuals can experience tremendous shifts in abiotic conditions. *Nematostella*'s infaunal distribution also may expose this species to various pollutants that concentrate into the sediment. Due to ease of laboratory culture through the full life cycle, tractability of genetic manipulations, and the availability of a sequenced genome *Nematostella* has become a cnidarian model for cellular and molecular responses to environmental stress (Goldstone, 2008; Reitzel et al., 2008; Tarrant et al., 2015). Given the limited information available on the global transcriptomic response to xenobiotic exposure in cnidarians, we sought to expand the understanding of cnidarian stress responses beyond the small number of well-characterized biomarkers. This approach provides an opportunity to investigate the potential of a taxonomically restricted response, which might be shared with corals or unique to this salt marsh resident. However, since *Nematostella,* as a cnidarian, belongs to a sister group to the Bilateria, characterization of these responses may also provide a way to root studies in bilaterian organisms (e.g., fish, oyster, shrimp) to assess conserved and divergent responses between vertebrates and invertebrates.

In this study we investigate the transcriptome-wide responses of *Nematostella* to dispersant and/or crude oil exposure alone, or coupled to a physical stressor (UV radiation). We hypothesized that sweet crude oil exposure would result in up-regulation of genes associated with xenobiotic metabolism and antioxidant defenses, and that co-exposure to dispersant and/or UV radiation would result in larger numbers of differentially expressed genes. Because we sought to gain mechanistic insight into both novel and conserved molecular responses, we conducted a gene-ontology (GO) enrichment analysis to identify regulated processes in an unbiased manner and also explicitly examined differential responses of genes with known or predicted roles in the stress response.

## 2. MATERIALS AND METHODS

### *2.1. Animal culture*

Adult *Nematostella* were originally collected from Great Sippewissett Marsh, MA USA and propagated in the laboratory over several years. Animals used in these experiments were reared for over one month in common garden at room temperature in glass dishes (12 x 18 x 5.5 cm) containing 500 ml filtered natural seawater, diluted to 20 ppt, referred to subsequently as "seawater" (<100 anemones, ~10 g total wet weight per container). Animals were fed brine shrimp nauplii four times per week, and water was changed weekly. Animals held in these conditions exhibit consistent growth and can be induced to spawn regularly (Reitzel et al. 2013, Stefanik et al. 2013).

### *2.2. Chemical and UV exposures*

For chemical exposures, a water accommodated fraction of Corexit® 9500 dispersant (referred to as DISP) and a water accommodated fraction of Macondo sweet crude oil (referred to as WAF) were prepared by adding dispersant or sweet crude oil into an amber-colored glass bottle containing diluted seawater to give nominal concentrations of DISP (100 ul dispersant diluted into 900 ml distilled water; 2 µl diluted dispersant added to 100 ml seawater; 2 ppm (v:v)) or oil (2 µl of sweet crude oil added to 100 ml seawater; 20 ppm (v:v)). To test for possible effects of Corexit® 9500 chemical dispersant and sweet crude oil, a chemically-enhanced WAF (referred to as CEWAF) was generated by creating a mixture of 2 ppm of dispersant and 20 ppm of sweet crude oil in seawater (2 ul of 1:10-diluted dispersant and 2 ul sweet crude oil added to 100 ml seawater). All three bottles (DISP, WAF and CEWAF) were capped tightly and stirred overnight with a Teflon-coated magnetic stir bar such that a vortex was formed that reached one-third of the way toward the bottom of the bottles (Tarrant et al., 2014). These chemical exposures are consistent with environmentally relevant concentrations (Hamdan and Fulmer, 2001) and are significantly lower than concentrations that have resulted in significant toxicity in other marine invertebrates (Goodbody-Gringley et al., 2013). Furthermore, the concentrations were chosen because they have previously resulted in measurable changes in gene expression (Tarrant et al., 2014).

UV radiation was provided by a UV-B-enriched bulb (Zilla Desert Series fluorescent T5 bulb, purchased at Petco (Falmouth, MA, USA). *Nematostella* were exposed to seawater (experimental control), three chemical treatments (DISP, WAF and CEWAF), seawater with UV

(referred to as UV), or three chemical treatments with the addition of UV (DISP_UV, WAF_UV and CEWAF_UV). For the experimental period, 3-4 adult *Nematostella* were placed into each of three glass dishes (30 mm diameter x 12 mm depth, Electron Microscopy Sciences, Hatfield, PA, USA) per treatment. Dishes were covered either with UV-transparent plastic (UV treatments) or with UV-opaque glass (no UV treatments). Dishes were incubated for 6 h on a shelf 14 cm below the UV bulb (providing 1.6 W $m^{-2}$ UV-A and 0.66 W $m^{-2}$ UV-B, measured using an OL 656 UV-vis spectroradiometer as in Tarrant et al. 2014). After 6 h, the UV bulb was turned off, and animals were sampled 18 h later (24 h after the start of the experiment). UV exposure conditions were primarily chosen because we have previously observed effects on gene expression in *Nematostella* with this level of exposure. While the levels are environmentally realistic (lower than noon levels on a cloudless day in July at 42°N), the levels experienced by natural populations of *Nematostella* are reduced to an unknown degree through burrowing into sediments (see Tarrant et al. 2014 for additional discussion).

All 8 combinations of controls and chemical and/or UV treatments were characterized by global transcriptional profiling (RNA-seq). At the end of the exposure periods, all animals were immediately placed in microcentrifuge tubes containing a 10-fold excess (w:v) of RNAlater using plastic transfer pipettes. Samples in RNAlater were gently inverted and stored at -20°C until total RNA isolation. Single biological replicates were generated by pooling all of the adult *Nematostella* from a single dish into one sample; thus, the three dishes in each treatment resulted in three biological replicates.

*2.3. Library preparation and next generation sequencing*

Total RNA was extracted from the pooled animals within each glass dish using the Aurum Fatty and Fibrous Tissue Kit (Bio-Rad, Hercules CA), according to the manufacturer's protocol, including DNAse treatment. RNA quantity and purity were assessed using a Nano Drop 1000 spectrophotometer (Thermo Scientific, Wilmington, DE, USA). Quality of the total RNA was confirmed prior to library preparation with an Agilent 2100 Bioanalyzer (Agilent Technologies, Santa Clara, CA) using the Agilent RNA 6000 Nano assay (average RNA Integrity Number (RIN) of 9.225; minimum RIN of 8.2 and maximum RIN of 9.7). The Illumina library preparation and sequencing was performed by the Genomics Service Laboratory at the HudsonAlpha Institute for Biotechnology (Huntsville, AL) using the HiSeq 2500 platform to generate a minimum target of 25 million, 50 base-pair, paired-end reads per sample. RNA-seq was performed on three individual biological replicates per control or treatment (total of 24 samples).

*2.4. Reference mapping, statistical analyses of differential expression and gene ontology enrichment*

The software pipeline optimized by Helm et al. (2013) was used for all reference mapping and statistical analysis of differential gene expression. A summary of the methods is included here, but all supplementary reference files, including source codes, are available through Helm et al. (2013). A reference transcriptome consisting of 26,514 transcripts, including the mitochondrial genome, and 18S and 28S ribosomal RNA, was used for mapping all reads that passed the Illumina chastity filter. The sequence reads were mapped using bowtie 2.2.0 with the following parameters: –very-sensitive-local (increases sensitivity at the cost of computational resources) and –a flags (returns all possible mappings for a single read). Counts were generated from the bowtie2 map file using the script generated by Helm et al. (2013). Any reads that mapped to more than one reference sequence were not counted, and multiple mappings to the same reference sequence are only counted once. The R library edgeR version 3.0.4 (Robinson et al., 2009) was used for determining the significance of the differential gene expression using the parameters as previously described (Helm et al., 2013). Differentially expressed genes were identified by comparing all seven chemical and/or UV treatments to the Seawater/No UV control. P-values were corrected for multiple testing using p.adjust and Bonferroni correction, and only genes with an adjusted p-value $\leq 0.05$ (equivalent to an unadjusted p-value $\leq 2.84 \times 10^{-6}$) and a fold change of $\geq 1.5$ were considered statistically significant.

Differentially expressed genes were analyzed using Gene Ontology (GO) annotations (cellular component, molecular function and biological processes) with GOseq version 1.10.1, a software package that performs GO enrichment analysis for RNA-seq data by properly incorporating the effect of selection bias (Young et al., 2010). GO term enrichment was determined by comparing the list of differentially expressed genes against all of the transcripts in the reference transcriptome. An adjusted p-value of $\leq 2 \times 10^{-4}$ was used as the cutoff for consideration of enrichment of the GO terms.

*2.5. Confirmation of differential gene expression by real-time RT-PCR*

An identical parallel experiment was conducted to provide material for RT-PCR measurements. For this, total RNA was extracted from the pooled animals within each glass dish and the quality of the total RNA was assessed as previously mentioned. cDNA was synthesized from 1 µg of total RNA in a 20 µl reaction using an iScript cDNA synthesis kit (Bio-Rad). Expression of genes of interest was measured using a MyCycler Real-Time PCR

detection system and a 20 µl reaction mixture consisting of 10 µl of SsoFast EvaGreen Supermix (Bio-Rad), 500 nmol $l^{-1}$ gene-specific primers and 0.8 µl of cDNA (0.25 µl in the 18S assay). Sequences of gene-specific primers were previously provided (Tarrant et al., 2014). Expression was calculated by comparing the threshold cycle of amplification against a standard curve constructed from a serially diluted plasmid standard containing the amplicon of interest. PCR conditions were as follows: 95°C for 2 min followed by 40 cycles of 95°C for 5 s and 60°C for 10 s. After 40 cycles, the products were subjected to melt curve analysis to ensure that only a single specific product was amplified.

Expression for each gene of interest was normalized to 18S expression, and fold-change was then calculated by dividing expression for each sample by the mean expression for the control (no UV or chemical exposure). Normality was evaluated by the Kolmogorov–Smirnov test, and equality of variance was evaluated through visual inspection of residuals. Data were either left untransformed or transformed by the square root or base-10 logarithm to satisfy these assumptions. Expression of each gene was analyzed using a two-way analysis of variance with UV exposure and chemical treatments as fixed factors. Posthoc comparisons for significant effects were conducted using Tukey's test. Transformation, evaluation of residuals and statistical tests were conducted using SYSTAT 13 (Systat Software Inc., Chicago, IL, USA).

## 3. RESULTS AND DISCUSSION

### *3.1. Sequencing and mapping coverage statistics*

A total of 812,627,568 PE DNA sequencing reads were generated from 24 samples (3 biological replicates, 8 treatments) from which an average overall alignment rate of 64.01 ± 0.96% (mean ± 1 standard deviation) per sample was achieved after quality filtering. This overall rate included alignments to protein-coding genes and the mitochondrial genome, as well as 18S and 28S ribosomal RNA. A summary of the total number of reads and the various alignments is provided in Supplemental Table 1. On average, ~16.35 million PE reads per sample aligned to protein coding genes, representing an average coverage of 48.3 ± 1.1% of reads. All Illumina read files have been deposited in the NCBI Sequence Read Archive (BioProject ID: PRJNA427809).

### *3.2. Nematostella exhibits modest molecular responses to oil and/or dispersant exposure*

We first assessed differential gene expression in response to water-accommodated fractions of dispersant (DISP), oil (WAF) or oil & dispersant (CEWAF) without any UV exposure. A

complete summary of results (including p-values, counts, fold change, and transcript and gene ontology annotations) is included as Supplementary File #1. The DISP treatment produced the strongest molecular response with a total of 91 transcripts differentially expressed, 6 up-regulated and 85 down-regulated (Figure 1A). Based on a comparison of all three treatments with the seawater control, a total of 12 transcripts were up-regulated in at least one of the three treatments while 98 transcripts were down-regulated (Figure 1B). DISP resulted in the up-regulation of 2 unique transcripts, while WAF resulted in the up-regulation of 6 unique transcripts. Of the remaining 3 transcripts, one was up-regulated in both DISP and WAF, while the last two were up-regulated in all three exposures. Interestingly, there was no overlap in down-regulated transcripts between all three exposures. DISP resulted in the strongest unique signature with a total of 74 unique transcripts down-regulated. These relatively modest changes in gene expression may appear to contrast with previous studies that have reported severe deleterious effects on corals (e.g., tissue mortality, reduced larval survival and settlement) following exposure to Corexit® 9500 dispersant (DeLeo et al., 2012; Goodbody-Gringley et al., 2013); however, these previous studies used much higher concentrations (35-100 ppm) than those used here (2 ppm). These differences in results and exposure conditions point to the need for more detailed dose-response studies; for cnidarians, such studies have only been conducted with other dispersants (e.g., Corexit® 9527; Venn et al. 2009).

The WAF treatment resulted in the differential expression of 25 transcripts (9 up-regulated and 16 down-regulated), while the CEWAF treatment produced the slightest change in gene expression with 11 transcripts differentially expressed (2 up-regulated and 9 down-regulated) (Figure 1A). Furthermore, WAF treatment resulted in the down-regulation of 4 unique transcripts, while CEWAF resulted in the down-regulation of 8 unique transcripts. Of the remaining 12 transcripts, 11 were up-regulated in both DISP and WAF, while the last one was up-regulated in WAF or CEWAF (Figure 1B). Thus, relative to dispersant alone *Nematostella* had minimal shifts in gene expression when exposed to WAF and surprisingly even fewer changes in gene expression in the combination treatment (CEWAF) (Figure 1). However, the low number of differentially expressed genes in response to WAF or CEWAF exposure is particularly important to note because similar exposures to crude oil in vertebrates have shown significantly greater numbers of differentially expressed genes (one or two orders of magnitude greater than observed in the current *Nematostella* data) (Zhu et al., 2016; Xu et al., 2016; Garcia et al., 2012). However, these large changes in gene expression in vertebrates result largely from the activation of the AHR pathway, as well as the significant amount of cross-talk with the NRF2 pathway (reviewed in Wakabayahi et al., 2010).

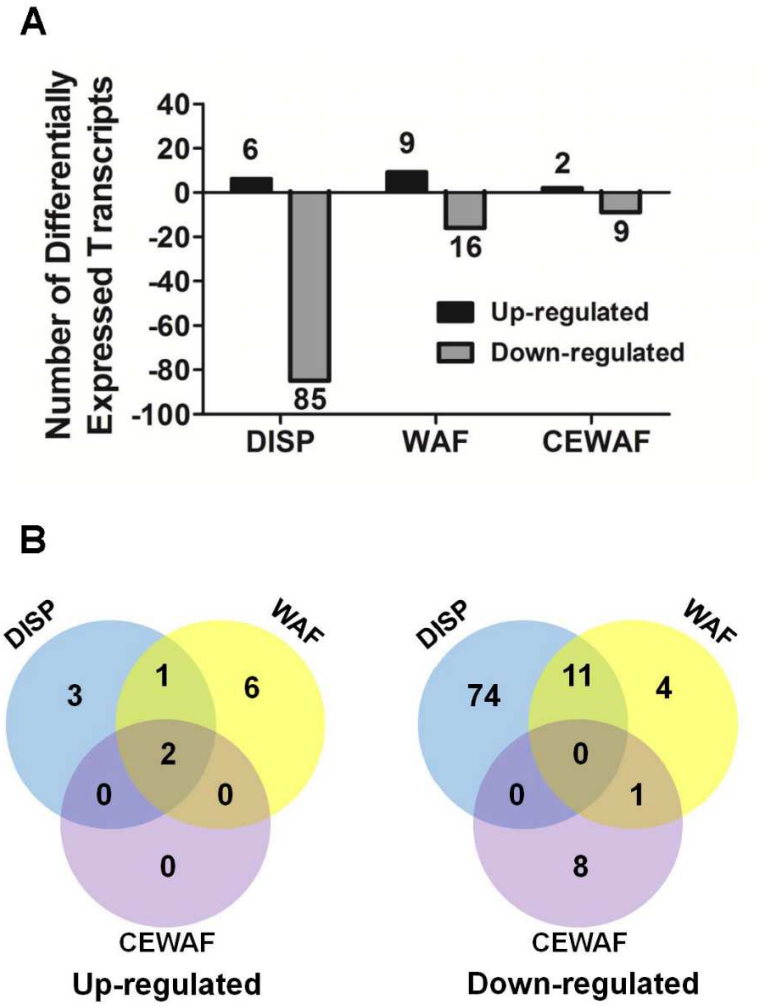


**Figure 1. Summary of differential gene expression in response to DISP, WAF and CEWAF exposure.** A) Total number of differentially expressed genes in response to DISP, WAF or CEWAF exposure for 24 hours (p-value ≤ 0.05 and a fold change of ≥ 1.5). B) Venn diagrams of differentially expressed genes up-regulated (left) or down-regulated (right) after exposure to DISP, WAF or CEWAF for 24 hours.

*3.3. UV exposure elicits a strong molecular response and synergizes the molecular response to dispersant and/or oil exposure*

We next evaluated changes in gene expression following exposure to dispersant and/or sweet crude oil in combination with a 6-hour UV exposure at the start of the 24-hour period. A complete summary of these results (including p-values, counts, fold change, and transcript and

gene ontology annotations) is included as Supplementary File #2. UV exposure resulted in a significant change in gene expression with a total of 605 transcripts being differentially expressed, 434 up-regulated and 171 down-regulated (Figure 2A). DISP_UV exposure resulted in the up-regulation of 480 transcripts and the down-regulation of 221 transcripts, while WAF_UV exposure resulted in an even stronger response with 541 and 248 transcripts up- or down-regulated, respectively. Finally, CEWAF_UV exposure produced the strongest response with 592 transcripts up-regulated, while 278 transcripts were down-regulated (Figure 2B).

A combined total of 1,133 unique transcripts were differentially expressed by all four UV treatments, 726 up-regulated and 407 down-regulated (Figure 2B). Of the 726 transcripts up-regulated by the combination of treatments, 292 transcripts were unique to DISP_UV, WAF_UV or CEWAF_UV exposure. Of the 434 transcripts up-regulated by UV exposure, only 21 were unique to UV exposure alone while 333 transcripts were up-regulated in all four UV treatment combinations. DISP_UV, WAF_UV and CEWAF_UV resulted in the up-regulation of 26, 50 or 89 unique transcripts, respectively, while 58 up-regulated transcripts were shared between DISP_UV, WAF_UV and CEWAF_UV. Of the total number of 407 transcripts down-regulated by all four UV treatment combinations, 236 transcripts were unique to DISP_UV, WAF_UV and CEWAF_UV exposure (Figure 2B). Of the 171 transcripts down-regulated by UV exposure, only 21 were unique to UV exposure alone while 103 transcripts were down-regulated in all four UV treatment combinations. DISP_UV, WAF_UV and CEWAF_UV exposure resulted in the down-regulation of 24, 56 or 57 unique transcripts, respectively, while 31 down-regulated transcripts were shared between DISP_UV, WAF_UV and CEWAF_UV treatments (Figure 2B).

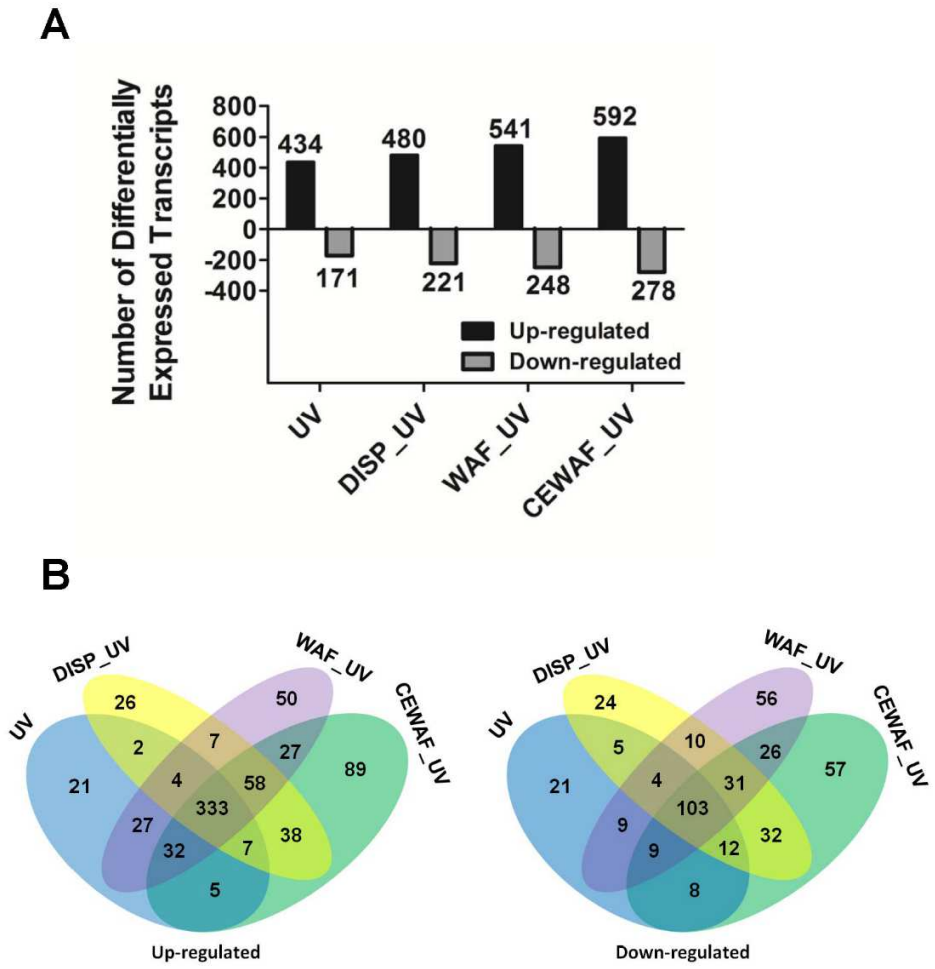


**Figure 2. Summary of differential gene expression in response to UV, DISP_UV, WAF_UV and CEWAF_UV exposure**. A) Total number of differentially expressed genes in response to UV, DISP_UV, WAF_UV or CEWAF_UV exposure (p-value ≤ 0.05 and a fold change of ≥ 1.5). B) Venn diagrams of differentially expressed genes up-regulated (left) or down-regulated (right) after exposure to UV, DISP_UV, WAF_UV or CEWAF_UV.

Expression patterns for four transcripts that were differentially expressed in the Illumina study were confirmed via real-time RT-PCR (Figure 3). In each case, a two-way ANOVA revealed a statistical interaction between responses to UV and chemical exposure. For one of the Cu/Zn SODs (v1g234825), post-hoc testing did not distinguish any statistically distinct comparisons, but all three Cu/Zn SODs showed the same pattern of up-regulation with UV

exposure alone or in the CEWAF_UV treatment. These results are consistent with the Illumina results: with both methods, three transcripts (the Cu/Zn SODs, Figures 3a-3c) were up-regulated in multiple UV treatments, and the Hsp70 transcript (Figures 3d) was down-regulated in several UV treatments.

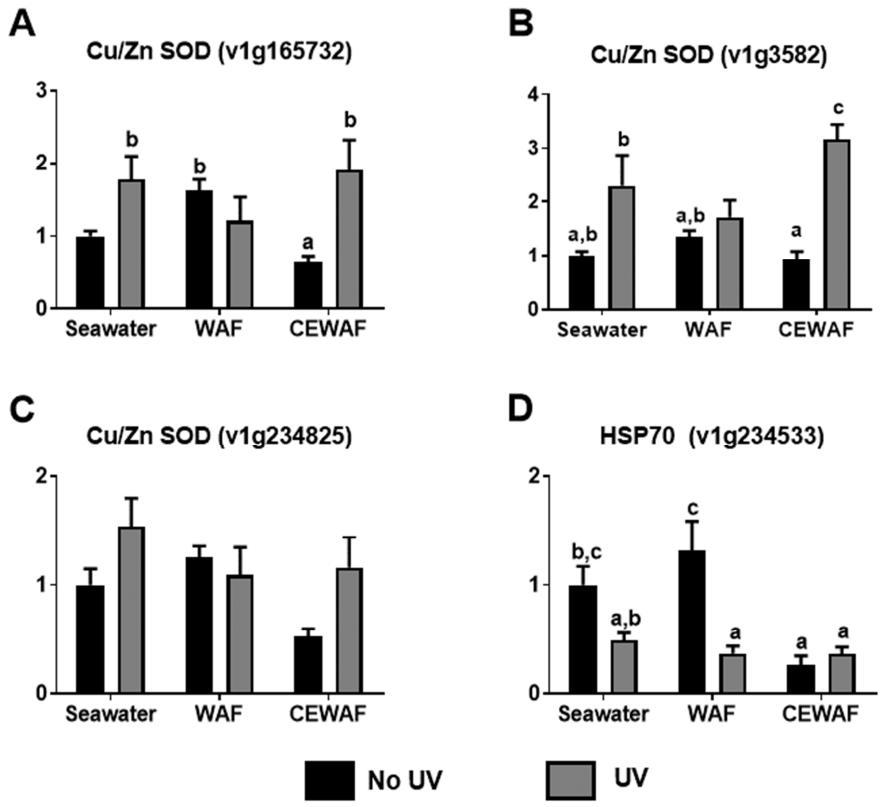


**Figure 3. Fold-change in gene expression from qPCR measurements of selected genes.** *Nematostella* were exposed to seawater alone, crude oil, or crude oil with dispersant. Grey bars indicate animals exposed to UV radiation, and black bars indicate no UV radiation. Data were analyzed using two-way ANOVA, and post-hoc analyses were conducted using Tukey's test. Different letters over bars indicate statistically different values. These genes correspond to (A) NvCuZnSOD2 (v1165732), (B) NvCuZnSOD3 (v1g3582), (C) NvCuZnSOD1 (v1g234825) and (D) NvHsp70 (v1g234533) from Tarrant et al. (2014).

To further investigate the functional annotation of differential gene expression in response to chemical and UV treatments, we performed a GO enrichment analysis to identify the GO categories that are overrepresented in the sets of differentially expressed transcripts. Due to the low number of differentially expressed transcripts, there were no significantly enriched GO categories in the DISP, WAF or CEWAF treatments. However, consistent with the observed

changes in differential gene expression, there was a concomitant increase in the total number of associated GO terms in the combined UV treatments that exhibited more robust changes in global transcript levels (Figure 4). A total of 33 GO categories were significantly enriched in the transcripts up-regulated in one or more of the UV treatments (Table 1), while a total of 23 GO categories were significantly enriched in the transcripts down-regulated by one or more of the four UV treatment combinations (Table 2).

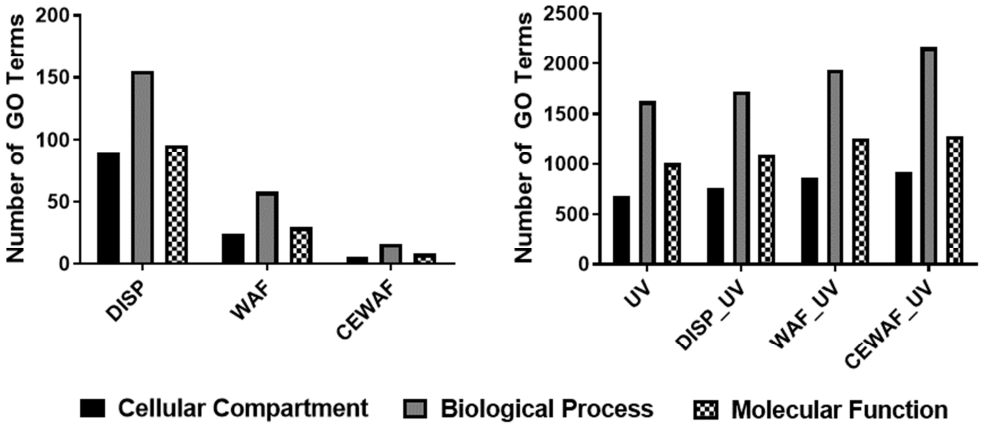


**Figure 4. Summary of the total number of gene ontology annotations from differentially expressed transcripts in response to cellular stress**.

Many of the enriched GO terms from all three functional categories are related to mitochondrial respiration (e.g., oxidative phosphorylation, mitochondrial electron transport, electron carrier activity, cytochrome-c oxidase activity, ubiquinone biosynthetic process). Additional GO categories in transcripts up-regulated by the various UV treatment combinations are consistent with effects on protein degradation and the unfolded protein response (e.g., chaperone binding, ATP-dependent peptidase activity, misfolded or incompletely synthesized protein catabolic process) (Table 1). Many of the GO categories enriched in down-regulated transcripts from the various UV treatment combinations are related to extracellular matrix components and functions that are consistent with basic morphogenetic and homeostatic roles, e.g., myosin filament assembly, calcium ion binding, extracellular matrix structural constituent, actin filament assembly and maintenance, and notochord morphogenesis and skeletal system development (Table 2).

Interestingly, our GO results for both the up- and down-regulated genes strongly mirrored experimental observations from a microarray analysis of normal human fibroblast cells exposed

to UV-B (Tsai et al., 2009). In this study, genes involved in protein turnover and mitochondrial respiration were up-regulated and genes involved in cytoskeletal structure and cellular adhesion were down-regulated. A second earlier microarray study utilizing primary human keratinocytes also observed the significant induction of genes related to proteasomal degradation and protein translation, while also observing the down-regulation of genes associated with cellular adhesion (Sesto et al., 2002). However, this particular oligonucleotide microarray only had coverage for 6,000 genes and there was no mention of genes involved in mitochondrial respiration. Furthermore, a related study utilizing primary murine fibroblast skin cells demonstrated that UV-B exposure resulted in a significant increase in the production of both superoxide anion radicals and hydrogen peroxide, most likely the result of increased mitochondrial respiration (Masaki and Sakurai, 1997). The later study by Tsai et al. (2009) confirmed that mitochondrial activity significantly increases in a time-dependent manner during continuous UV-B exposure.

467 **Table 1. Gene Ontology Enrichment Summary for Up-Regulated Genes**

| Gene Ontology | GO Accession # | Description | UV | DISP_UV | WAF_UV | CEWAF_UV |
|---|---|---|---|---|---|---|
| Cellular Component | GO:0005739 | mitochondrion | 1.05E-15 | 7.42E-13 | 2.10E-15 | 2.76E-14 |
| Cellular Component | GO:0005743 | mitochondrial inner membrane | 8.70E-10 | 2.69E-08 | 4.76E-09 | 4.88E-09 |
| Cellular Component | GO:0005759 | mitochondrial matrix | 5.51E-08 | 7.43E-06 | 1.08E-08 | 1.63E-06 |
| Cellular Component | GO:0045277 | respiratory chain complex IV | 1.47E-05 | 8.88E-07 | 3.81E-05 | 5.64E-05 |
| Cellular Component | GO:0031966 | mitochondrial membrane | 2.93E-04 | 2.74E-06 | NA | 9.20E-06 |
| Cellular Component | GO:0042645 | mitochondrial nucleoid | NA | 6.96E-05 | 1.16E-04 | NA |
| Biological Process | GO:0055114 | oxidation-reduction process | 3.37E-11 | 2.34E-09 | 5.67E-11 | 4.35E-10 |
| Biological Process | GO:0008535 | respiratory chain complex IV assembly | 1.27E-07 | 2.04E-07 | 3.29E-07 | 5.13E-07 |
| Biological Process | GO:0015992 | proton transport | 1.68E-07 | 4.55E-08 | 8.91E-06 | 2.65E-06 |
| Biological Process | GO:0006744 | ubiquinone biosynthetic process | 5.29E-07 | 1.08E-06 | 2.67E-05 | 4.30E-06 |
| Biological Process | GO:0016226 | iron-sulfur cluster assembly | 2.51E-06 | 1.22E-04 | 6.63E-06 | 2.49E-04 |
| Biological Process | GO:0022904 | respiratory electron transport chain | 8.77E-06 | 1.39E-05 | 2.26E-05 | 3.40E-05 |
| Biological Process | GO:0006123 | mitochondrial electron transport, cytochrome c to oxygen | 5.17E-05 | 4.42E-06 | 1.32E-04 | 1.94E-04 |
| Biological Process | GO:0006637 | acyl-CoA metabolic process | 4.89E-05 | NA | 1.17E-04 | NA |
| Biological Process | GO:0006119 | oxidative phosphorylation | 2.04E-04 | NA | 6.84E-05 | NA |
| Biological Process | GO:0006515 | misfolded or incompletely synthesized protein catabolic process | 2.43E-04 | NA | NA | NA |
| Biological Process | GO:0007006 | Mitochondrial membrane organization | NA | NA | 1.54E-04 | NA |
| Molecular Function | GO:0051087 | chaperone binding | 1.62E-04 | 2.88E-05 | 5.17E-06 | 9.22E-05 |
| Molecular Function | GO:0050660 | flavin adenine dinucleotide binding | 8.01E-16 | 7.41E-12 | 2.45E-16 | 2.30E-12 |
| Molecular Function | GO:0051537 | 2 iron, 2 sulfur cluster binding | 1.12E-10 | 2.76E-06 | 1.66E-08 | 3.64E-08 |
| Molecular Function | GO:0009055 | electron carrier activity | 2.65E-09 | 7.35E-08 | 7.10E-08 | 7.39E-08 |
| Molecular Function | GO:0003995 | acyl-CoA dehydrogenase activity | 2.52E-08 | 3.49E-05 | 8.75E-08 | 8.35E-05 |
| Molecular Function | GO:0004176 | ATP-dependent peptidase activity | 1.27E-07 | 2.04E-07 | 3.23E-07 | 5.13E-07 |
| Molecular Function | GO:0003904 | deoxyribodipyrimidine photo-lyase activity | 4.38E-07 | 3.55E-05 | 1.36E-08 | 7.33E-05 |
| Molecular Function | GO:0051539 | 4 iron, 4 sulfur cluster binding | 1.43E-06 | 2.72E-06 | 6.39E-05 | 9.12E-06 |
| Molecular Function | GO:0004129 | cytochrome-c oxidase activity | 3.53E-05 | 2.73E-06 | 9.08E-05 | 1.34E-04 |
| Molecular Function | GO:0051082 | unfolded protein binding | 8.01E-05 | 1.88E-04 | 9.47E-05 | 2.30E-04 |
| Molecular Function | GO:0050662 | coenzyme binding | 1.37E-04 | 2.13E-04 | NA | NA |
| Molecular Function | GO:0009055 | electron carrier activity | 2.65E-09 | 7.35E-08 | 7.10E-08 | NA |
| Molecular Function | GO:0010181 | FMN binding | 3.79E-04 | NA | 2.09E-06 | NA |
| Molecular Function | GO:0046872 | metal ion binding | NA | 8.95E-05 | NA | 1.08E-06 |
| Molecular Function | GO:0005506 | iron ion binding | NA | NA | 2.26E-04 | NA |
| Molecular Function | GO:0003914 | DNA (6-4) photolyase activity | NA | NA | 1.73E-04 | NA |

468 **Table 2. Gene Ontology Enrichment Summary for Down-Regulated Genes**

| Gene Ontology | GO Accession # | Description | UV | DISP_UV | WAF_UV | CEWAF_UV |
|---|---|---|---|---|---|---|
| Cellular Component | GO:0044420 | extracellular matrix component | 7.69E-09 | 2.95E-08 | 3.90E-08 | 7.21E-08 |
| Cellular Component | GO:0005581 | collagen trimer | 1.63E-10 | 4.30E-14 | 1.33E-13 | 5.64E-13 |
| Cellular Component | GO:0005578 | proteinaceous extracellular matrix | 8.83E-09 | 4.34E-10 | 1.61E-08 | 5.16E-09 |
| Cellular Component | GO:0001527 | microfibril | NA | 2.10E-05 | 2.54E-05 | NA |
| Cellular Component | GO:0005604 | basement membrane | NA | 4.38E-07 | 7.46E-07 | NA |
| Cellular Component | GO:0005576 | extracellular region | NA | 6.83E-06 | NA | 1.59E-05 |
| Biological Process | GO:0010466 | negative regulation of peptidase activity | 5.77E-06 | 2.32E-08 | 1.21E-06 | 1.01E-07 |
| Biological Process | GO:0048570 | notochord morphogenesis | 1.23E-05 | 2.62E-05 | 3.42E-05 | NA |
| Biological Process | GO:0031034 | myosin filament assembly | 5.34E-06 | 1.10E-05 | NA | 2.09E-05 |
| Biological Process | GO:0042063 | gliogenesis | NA | NA | NA | 5.00E-05 |
| Biological Process | GO:0001501 | skeletal system development | NA | 4.66E-05 | 7.14E-05 | NA |
| Biological Process | GO:0072358 | cardiovascular system development | NA | 3.13E-05 | 4.81E-05 | NA |
| Biological Process | GO:0030198 | extracellular matrix organization | NA | 3.95E-05 | NA | 1.08E-04 |
| Biological Process | GO:0030043 | actin filament fragmentation | NA | 8.98E-05 | NA | NA |
| Biological Process | GO:0051014 | actin filament severing | NA | 1.41E-04 | NA | NA |
| Biological Process | GO:0045010 | actin nucleation | NA | 8.73E-05 | NA | NA |
| Biological Process | GO:0035583 | sequestering of TGFβ in extracellular matrix | NA | 2.02E-04 | NA | NA |
| Biological Process | GO:0009987 | cellular process | NA | 5.12E-06 | NA | NA |
| Biological Process | GO:0048477 | oogenesis | NA | NA | 9.16E-05 | NA |
| Molecular Function | GO:0030414 | peptidase inhibitor activity | 5.94E-06 | 2.30E-08 | 1.20E-06 | 1.01E-07 |
| Molecular Function | GO:0005201 | extracellular matrix structural constituent | 4.28E-15 | 2.51E-23 | 1.22E-20 | 6.49E-20 |
| Molecular Function | GO:0005509 | calcium ion binding | 8.53E-06 | 1.41E-06 | 5.92E-07 | 1.29E-04 |
| Molecular Function | GO:0005488 | binding | NA | NA | NA | 4.58E-05 |

469

470

471 *3.4. Nematostella defensome response*

472 We next specifically examined differential responses of genes with known or predicted roles
473 in the stress response (Figure 5), including members of the *Nematostella* defensome
474 (Goldstone, 2008), components of the shikimate synthesis pathways (Starcevic et al., 2008;
475 Shinzato et al., 2011), and genes differentially expressed following exposure to metals (Elran et
476 al., 2014). We observed differential expression of many classic stress response genes between

the various UV treatments, as well as the expression of some novel cellular antioxidants and genes involved in the synthesis of UV protective compounds (Figure 5).

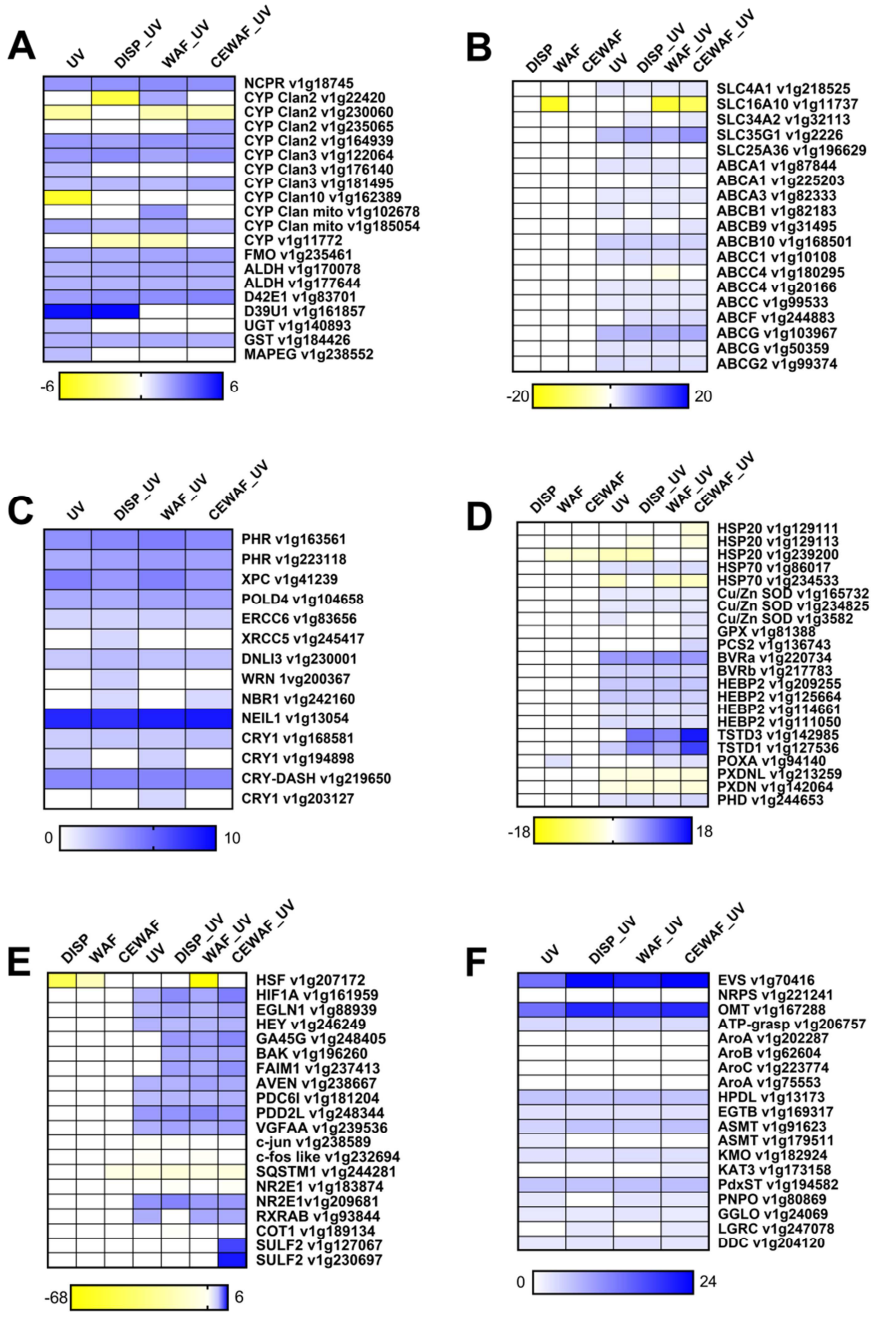


**Figure 5. Heat map of the *Nematostella* "defensome" response to cellular stress.** The "defensome" is being represented by six groups: A) phase I and phase II metabolic enzymes, B) membrane transporters, C) DNA repair enzymes, D) general stress response genes, E) cellular signaling proteins, and F) proteins involved in the production of UV protective compounds and

cellular antioxidants. Fold change is based on a log2 scale. Blue: up-regulated genes, yellow: down-regulated genes.

*3.4.1. Differential expression of genes involved in xenobiotic metabolism and membrane transport*

Although the AHR pathway is well characterized in vertebrates and AHR/ARNT genes have been identified in diverse invertebrate groups (Goldstone et al., 2006; Liu et al., 2010; Reitzel et al., 2014; Jenny et al., 2016), previous studies have suggested the lack of an AHR-dependent response to hydrocarbon exposure in multiple invertebrate species (reviewed in Hahn et al., 2017). While an AHR gene has been identified in *Nematostella*, the NvAHR protein fails to bind prototypical AHR ligands and shows no sign of physical interaction with the NvARNT protein (Reitzel et al., 2014). Furthermore, there is no evidence in the *Nematostella* genome of a CYP1A gene, although a large number of other CYP genes belonging to the xenobiotic-metabolizing Clans 2 through 4 are present (Reitzel et al., 2008; Goldstone, 2008). Even with this in mind, we were surprised that a number of specific classes of genes expected to be up-regulated with any xenobiotic exposure, such as phase I and II enzymes, were strongly up-regulated in the UV alone treatment (Figure 5A and 5B). Several cytochrome P450 (CYP) genes, mostly in Clans 2 and 3, as well as NADPH- cytochrome P450 reductase (NCPR) were induced by one or more of the UV treatments, but there was little evidence of additive or synergistic changes in the expression levels between the combined UV treatments. Of the 11 CYP genes differentially expressed, 4 of them were down-regulated in one more of the UV treatments. The only divergent change in CYP expression was observed with one CYP Clan 2 gene (v1g22420) which was down-regulated in the DISP_UV treatment, but up-regulated in the WAF_UV treatment. Other phase I enzymes, such as the flavin-dependent monooxygenase (FMO), two aldehyde dehydrogenase (ALDH) genes and short-chain dehydrogenases (D42E1 and D39U1) were also strongly induced in all four UV treatments. Finally, three phase II conjugating enzymes belonging to the GST and UDPGT were differentially expressed, with the UDPGT and one GST transcript significantly up-regulated only in the UV treatment, while a second GST transcript was significantly up-regulated in all four UV treatments (Figure 5A).

Although previous studies have demonstrated the up-regulation of CYP1 genes in vertebrates in response to UV-B exposure, this activation is mediated through the AHR-dependent binding of the UV-B activated tryptophan photoproduct 6-formylindolo[3,2-b]carbazole (FICZ) (Wei et al., 1998; Wei et al., 1999; Fritsche et al., 2007). Interestingly, a large repertoire of Clan 2 and Clan 3 CYP genes has been demonstrated to be up-regulated in

518 the copepod (*Tigriopus japonicas*) in response to UV-B exposure (Puthumama et al., 2017). At
519 this time we have no specific mechanism to explain the induction of invertebrate CYP genes in
520 response to UV treatment, but other transcription factors such as the nuclear receptor
521 hepatocyte nuclear factor 4α (HNF4α, NR2A1), as well as pregnane X receptor (PXR) and
522 constitutive androstane receptor (CAR) play major roles in the regulation of CYP2 and CYP3
523 genes (Tirona et al., 2003; Chen et al., 2005; Jover et al., 2009) in vertebrates. Thus similar
524 nuclear receptors may play a role in the regulation of invertebrate CYP genes in response to
525 cellular stress. These current data do highlight the utility of investigations in early diverging
526 animal phyla to achieve a greater understanding of the evolution of transcriptional regulation of
527 the stress response in metazoans.
528 Several solute carrier and ABC transporter transcripts significantly induced by one or more
529 of the UV treatment combinations (Figure 5B). A total of 10 transcripts encoding solute carriers
530 or ABC transporters were induced in all four UV treatment combinations, with no sign of any
531 significant difference between treatments. Interestingly, previous studies have demonstrated
532 the induction of ATP-binding cassette (ABC) transporters in response to UV exposure (Uchiumi
533 et al., 1993; Hu et al., 2000). Furthermore, ABC transporters have been demonstrated to play a
534 protective role in developing sea urchins exposed to UV-B (Leite et al., 2014). A single solute
535 carrier, SLC35G1, encoding a putative calcium-transporting ATPase was induced in all four UV
536 treatment combinations, but the induction was modestly enhanced in DISP_UV, WAF_UV and
537 CEWAF_UV, resulting in a ~1.5 to 1.8-fold increase in transcript abundance. Two additional
538 solute carriers (SLC34A2 and SLC25A36) were not induced by UV treatment alone, but were
539 induced by DISP_UV exposure, while SLC34A2 was also induced by CEWAF_UV exposure.
540 Finally, a copy of an ABCA1 transcript, as well as copies of ABCB9 and ABCF transcripts, were
541 not induced by UV treatment alone, but were induced by UV treatment combined with one or
542 more dispersant and/or oil exposures (Figure 5B). The induction of these transporters in the
543 combined UV treatments is indicative of enhance toxicity of photo-activated hydrocarbons and is
544 consistent with their functions in the cellular export of xenobiotics.
545
546 *3.4.2. Differential expression of genes involved in DNA repair*
547 One of the most common forms of cellular damage associated with UVB exposure is the
548 formation of cyclobutane pyrimidine dimers (CPDs), which results in the covalent linking
549 between pairs of thymine or cytosine bases on the same strand of DNA through the formation of
550 a cyclobutane bridge (Niggli and Cerutti, 1983; Douki and Cadet, 2001). A second common
551 type of DNA lesions associated with UVB exposure are pyrimidine-pyrimidone (6-4)

552 photoproducts, although the relative abundance of CPDs and (6-4) photoproduct formation is
553 dependent on specific wavelengths (Matsunaga et al., 1991). Two transcripts (v1g163561 and
554 v1g223118) encoding deoxyribodipyrimidine photolyases were consistently up-regulated in all
555 four UV treatments (Figure 5C). The photolyase/cryptochrome superfamily of proteins,
556 recognized by the conserved photolyase homology region (PHR) domain, represents a group of
557 photoreceptor proteins that play various roles in DNA repair and regulation of circadian rhythms
558 (reviewed in Sancar, 2003). Deoxyribodipyrimidine photolyases are light-dependent DNA-repair
559 enzymes that remove these UV-light induced lesions through the process of photoreactivation.
560 They contain a two-electron reduced flavin $FADH^-$ cofactor that is activated by light energy and
561 serves as an electron donor to the pyrimidine dimer resulting in a radical anion that splits into
562 two pyrimidines (reviewed in Sancar, 2003).
563 Differential expression was also observed for several cryptochrome/photolyase members;
564 for these genes, more detailed phylogenetic analyses have been conducted, leading to
565 supplementary annotations (Reitzel et al., 2010; Shoguchi et al., 2013). Two transcripts
566 encoding cryptochrome family members (CRY1 v1g168581 = NvCry1a; CRY1 v1g194898 =
567 CRY-DASH-like) were induced in all four combined UV treatments, while a third cryptochrome
568 (v1g219650 = NvCry2) transcript was only induced in the UV or WAF_UV treatments and a final
569 family member (v1g203127 = 6-4 photolyase-like) was only induced in the WAF_UV treatment.
570 (Figure 5C). Cry-DASH proteins also have the conserved PHR domain found in both
571 photolyase and cryptochrome proteins. Although the significant enrichment of the GO
572 annotation for deoxyribodipyrimidine photolyase activity (Table 1) was observed in all four UV
573 treatment combinations, the enrichment of a related molecular function, DNA (6-4) photolyase
574 activity, in the WAF_UV treatment is directly related to the differential gene expression of
575 multiple cryptochrome transcripts (Figure 5C). While, cryptochromes are believed to no longer
576 play a role in eukaryotic DNA repair; Cry-DASH proteins retain some DNA repair ability
577 (reviewed by Chaves et al., 2011).
578 Additional differentially expressed genes include those involved in nucleotide excision repair
579 (XPC, ERCC6) and base excision repair (NEIL1), as well as two enzymes involved in DNA
580 replication and double-strand break repair via nonhomologous end joining transcripts (XRCC5
581 and WRN) which were only induced in the DISP_UV treatment (Figure 5C). While nucleotide
582 excision repair enzymes are also associated with the repair of bulky DNA lesions such as CPDs
583 and (6-4) photoproducts (Shah and He, 2015), the induction of the other types of DNA repair
584 enzymes may be indicative of other types of oxidative damage to nucleotide bases (Shafirovich
585 et al., 2016).

586

587 *3.4.3. Differential expression of genes involved in general stress response and cell signaling*

588 UV treatment alone or combined with dispersant and/or oil treatment did result in the
589 induction of some classic oxidative stress-response genes, including a single heat shock protein
590 70 transcript (HSP70) and multiple copper/zinc superoxide dismutases (Cu/Zn SODs) (Figure
591 5D), consistent with our previous findings (Tarrant et al., 2014). However, we also observed the
592 down-regulation of a second HSP70 transcript, as well as multiple HSP20 transcripts, in multiple
593 treatments (Figure 5D). Interestingly, a single glutathione peroxidase (GPX) transcript and
594 transcript encoding a phytochelatin synthase enzyme (PCS2) were only induced in the
595 CEWAF_UV treatment. UV treatment alone or combined with dispersant and/or oil treatment
596 also resulted in the induction of multiple transcripts encoding proteins involved in heme
597 homeostasis, including biliverdin reductase A (BVRA), biliverdin reductase B (BVRB), and
598 multiple heme-binding proteins (HEBP2). Combined chemical and UV exposure resulted in a
599 synergistic induction, 4-fold and 16-fold, of two transcripts encoding thiosulfate
600 sulfurtransferases, TSTD1 and TSTD3 respectively, in the CEWAF_UV treatment. We also
601 observed a significant up-regulation of the pleckstrin homology domain transcript (PHD)
602 previously identified as a potential stress response gene by Elran et al. (2014). Finally, two
603 peroxidasin transcripts (PXDN and PXDNL) were significantly down-regulated in all four UV
604 treatments, while a peroxinectin transcript (POXA) was up-regulated in the WAF_UV and
605 CEWAF_UV treatments (Figure 5D). Peroxidasin is a heme-containing peroxidase enzyme that
606 is involved with extracellular matrix formation (Papageorgiou and Heymans, 2014), while
607 peroxinectin is cellular adhesion protein (Lin et al., 2007). The altered expression of these
608 genes is consistent with the significant enrichment of GO terms involved in extracellular matrix
609 and morphogenesis (Table 2).

610 We observed differential expression in several genes related to cell signaling pathways,
611 many of which play prominent roles in the stress response (Figure 5E). Most interesting was
612 the down-regulation of heat shock factor (HSF), the transcription factor responsible for
613 regulating transcription of heat shock genes, in three different treatments (DISP, WAF, and
614 WAF_UV). Hypoxia inducible factor 1-alpha (HIF1A) was induced in all four UV treatments, and
615 there was an enhanced induction (1.5- to 1.7-fold increase) in the DISP_UV and CEWAF_UV
616 treatments. Furthermore, the hypoxia-inducible vascular endothelial growth factor A (VGFAA),
617 as well as the HIF1A regulatory enzyme Egl nine homolog 1 (EGLN1), were also induced in all
618 four UV treatment combinations. Two transcripts encoding extracellular sulfatase 2 (SULT2), an
619 enzyme that modulates signaling molecule binding sites on heparin sulfate proteoglycans, were

strongly induced in CEWAF_UV. Sequestosome-1 (SQSTM1), a cargo protein involved in selective autophagy, was significantly induced in the CEWAF treatment, as well as all four UV treatment combinations. While UV exposure alone was not enough to induce a significant change in expression, UV exposure combined with dispersant and/or oil treatment did result in the significant induction of growth arrest and DNA damage-inducible protein GADD45 gamma (GA45G), as well as two transcripts encoding proteins involved in apoptotic signaling (Bcl-2 homologous antagonist/killer, BAK; Fas apoptotic inhibitory molecule 1, FAIM1). Three additional transcripts encoding proteins involved in apoptotic cell death (cell death regulator AVEN; programmed cell death 6-interacting protein, PDC6I; programmed cell death 2-like, PDD2L) were up-regulated in all four UV treatments. Surprisingly, transcripts encoding putative c-fos and c-jun, two proteins that dimerize together to form the UV-responsive AP-1 transcription factor, were down-regulated in some of the UV treatment combinations. Finally, differential expression of multiple nuclear receptors (NR2E = NvNR6, a TLL subfamily member; COT1 = NvNR10, COUP-TF-like; RXRAB = NvNR2, a cnidarian-specific subfamily member) and other nuclear transcription factors (HEY) was observed in multiple UV treatments (Figure 5F; supplemental annotation of nuclear receptors based on Reitzel and Tarrant, 2009). The "HEY" transcript corresponds to a basic-helix-loop-helix family member (Hes/Hey-like) that has a strong diel expression pattern in both *Nematostella* and the coral *Acropora millepora* (Oren et al., 2015).

*3.4.4 Differential expression of a gene involved in the production of novel cellular antioxidants*

The ergothioneine biosynthesis protein 1-like (EGTB) transcript (v1g169317), up-regulated in all four UV-related treatments (Figure 5F), is an interesting gene for future research consideration. Ergothioneine is an alternative amino acid with putative antioxidant effects (Paul and Snyder, 2010). The Joint Genome Institute (JGI) Genome Portal for *Nematostella* currently has this gene annotated as sulfatase-modifying factor enzyme 1 (SUMF1). However, the highest BLAST results for this protein yield matches to sequences annotated as EGTB-like proteins, but the protein also has two conserved domain regions. While the C-terminal region contains a methyltransferase domain with strongest homology to a putative 4-mercaptohistidine N1-methyltransferase (ovoA_Cterm), the N-terminal region of the protein shares homology to the SUMF1/formylglycine-generating enzyme (YfmG) domain, as well as a 5-histidylcysteine sulfoxide synthase (ovoA_Nterm) domain. Comparisons of EGTB proteins also show similarity between the sulfoxide synthase domain of EGTB and the YfmG domain in the *Nematostella* EGTB-like protein (v1g169317). As previously mentioned, ergothioneine is an alternative amino

654 acid with putative antioxidant effects (Paul and Snyder 2010). However, the EGTB enzymes
655 are generally thought to be restricted to microorganisms such as fungi, bacteria and
656 cyanobacteria. Thus, if the *Nematostella* gene did indeed encode an EGTB enzyme, it would
657 likely represent another example of horizontal gene transfer. This gene is located on scaffold
658 124 of the *Nematostella* genome and contains many introns, as well as a GC content of 49%
659 which is consistent with the 47% GC content of the overall genome. Thus, this gene does
660 appear to be a true nuclear encoded gene and not a contaminating sequence from any potential
661 proteobacterial endosymbiont. Furthermore, the highly conserved ovoA_Nterm and
662 ovoA_Cterm domains within this protein suggest that it could very well be a 5-histidylcysteine
663 sulfoxide synthase enzyme involved in ovothiol biosynthesis (Braunshausen and Seebeck,
664 2011), and this is further supported by the 47% shared protein sequence identity to a 5-
665 histidylcysteine sulfoxide synthase enzyme from the sea urchin *Paracentrotus lividus*
666 (Castellano et al., 2016) identified by BLASTp analysis. The strong homology between the
667 ergothioneine and ovothiol synthesizing enzymes is explained by the observation that both
668 compounds are thiol-histidine natural products that are formed from the oxidative coupling of
669 cysteine to histidine or a histidine derivative, respectively, with reactions catalyzed by sulfoxide
670 synthase domains (Song et al., 2013; Mashabela and Seebeck, 2013; Goncharenko et al.,
671 2015). Ovothiols are mercaptohistidine molecules with very strong reducing antioxidant
672 functions, and are commonly found in the eggs, ovaries and biological fluids of marine
673 invertebrates (Turner et al., 1987; Castellano et al., 2016), and have been demonstrated to
674 protect sea urchin eggs from the oxidative stress associated with the respiratory burst of
675 fertilization (Turner et al., 1986; Shapiro and Turner, 1988). The induction of this transcript in all
676 four UV treatments supports previous observations of ovothiol induction in response to cellular
677 stress (Castellano et al., 2016) and suggests a more expanded role as a cellular antioxidant.
678
679 *3.4.5. Expression of genes involved in the production of UV-protective compounds*
680 One of the most interesting observations was the induction of transcripts encoding putative
681 proteins related to amino acid synthesis and metabolism, as well as vitamin B6 biosynthesis
682 (Figure 5F). Of particular interest was the very strong induction of several enzymes that
683 participate in the shikimic acid pathway, which is involved in the biosynthesis of aromatic amino
684 acids (phenylalanine, tyrosine and tryptophan) in microorganisms, fungi and plants, and
685 biosynthesis of UV-protective mycosporine-like amino acids (MAAs). MAAs are small water-
686 soluble compounds derived from aromatic amino acids that are capable of absorbing UVA and
687 UVB radiation, and they have also been implicated in roles as cellular antioxidants (reviewed by

688 Shick and Dunlap, 2002, Oren and Gunde-Cimerman, 2007). Aromatic amino acids and MAAs
689 in metazoans, including marine organisms, are generally hypothesized to be of dietary origin
690 since most metazoans lack genes coding for the enzymes of the shikimic acid pathway.
691 However, previous studies suggest that cnidarians, including nonsymbiotic corals and
692 anemones, are capable of synthesizing these essential amino acids (Fitzgerald and Szmant,
693 1997; Shick et al., 2002; Starcevic et al., 2008). Starcevic et al. (2008) provided evidence for
694 the horizontal transfer of both bacterial and dinoflagellate ancestral genes of the shikimic acid
695 pathway into the genome of *Nematostella*. Of those genes, 3-dehydroquinate synthase (DHQS;
696 v1g70416), the enzyme responsible for catalyzing the second step of the shikimic acid pathway,
697 was significantly up-regulated by UV treatment and this up-regulation was significantly
698 enhanced with DISP_UV, WAF_UV and CEWAF_UV treatments (Figure 5F). However, the
699 remaining genes encoding a chorismate synthase (AroC, v1g223774), two 5-
700 enolpyruvylshikimate-3-phosphate (EPSP) synthases (AroA, v1g202287; AroA, v1g75553), and
701 a second DHQS-like transcript (AroB, v1g62604) did not significantly change in expression.
702 Despite recent evidence that some genes in the *Nematostella* genome assembly likely resulted
703 from bacterial contamination (Artamonova and Mushegian, 2013), AroA and AroB are well
704 supported as real products of horizontally transferred. AroC is more likely to be a bacterial
705 contamination.
706 While DHQS participates in the synthesis of the aromatic amino acids, it also plays a
707 significant role in the synthesis of shinorine, a photo-protective MAA (Rahman et al., 2014).
708 Interestingly, a second route for MAA biosynthesis relies on the conversion of the metabolites of
709 the pentose-phosphate pathway, specifically sedoheptulose 7-phosphate to 4-deoxygadusol,
710 which serves as a precursor of MAAs (Balskus and Walsh, 2010). Shinzato et al. (2011)
711 demonstrated that both *Acropora digitifera* and *Nematostella* contain homologs of a four-gene
712 cluster of enzymes (DHQS, O-MT, ATP-grasp, NRPS) also found in the cyanobacterium
713 *Anabaena variabilis* which is sufficient for the conversion of pentose-phospate metabolites to
714 shinorine. Three of those four genes were significantly up-regulated in all four UV-related
715 treatments. In addition to the previously discussed DHQS transcript, we also observed the
716 significant induction of the O-methyltransferase transcript (O-MT; v1g167288) in all four UV
717 treatments (Figure 5F). The DHQS and O-MT proteins have been demonstrated to work
718 together to convert sedoheptulose 7-phosphate into 4-deoxygadusol (Balskus and Walsh,
719 2010). We also observed the significant induction of a transcript (v1g206757) encoding an
720 enzyme in the ATP-grasp superfamily (Figure 5F), which include proteins that catalyze the ATP-
721 assisted kinase/ligase reaction of carboxylic acid with a nucleophile to produce an

722 acylphosphate intermediate (reviewed in Fawaz et al., 2011). The ATP-grasp enzyme homolog
723 in cyanobacteria has been demonstrated to be capable of converting 4-deoxygadusol and
724 glycine into mycosporine glycine (Balskus and Walsh, 2010). In contrast, we did not observe
725 induction of the nonribosomal peptide-synthetase (NRPS)-like transcript (v1g221241), which
726 putatively encodes an enzyme that is capable of converting mycosporine glycine and serine into
727 shinorine (Balskus and Walsh, 2010). However, we did observe induction of a linear gramicidin
728 synthase subunit C (LGRC) transcript (v1g247078), which has some homology to the NRPS-like
729 gene in *Hydra magnipapillata*, in the DISP_UV and CEWAF_UV treatments. Interestingly, both
730 of these genes (v1g221241 and v1g247078) contain a conserved adenylation domain found in
731 NRPS proteins (A_NRPS domain). However, the top BLASTp results of the putatively encoded
732 NRPS-like protein (v1g221241) demonstrated strong homology (50-70% identity) to linear
733 gramicidin synthase subunit D-like genes from several different invertebrate species, including
734 genes from multiple cnidarian species, e.g., *Acropora digitifera, Orbicella faveolata* and
735 *Exaiptasia pallida*. In contrast, the top BLASTp results of the LGRC sequence (v1g247078) had
736 the strongest homology (33-38% identity) to NRPS proteins of bacterial origin. Taken together,
737 these data suggest that *Nematostella* is capable of synthesizing MAAs as a protective
738 mechanism in response to cellular stress. However, some exciting questions remain regarding
739 whether or not the potential synthesis of these MAAs is primarily driven by genes encoded in
740 the *Nematostella* genome due to horizontal gene transfer, the result of gene expression from a
741 proteobacterial endosymbiont, or some form of symbiotic interplay between *Nematostella* and a
742 proteobacterial endosymbiont.
743 Some additional supporting evidence for the *de novo* synthesis of MAAs in *Nematostella* is
744 present in the induction of other genes related to amino acid metabolism and vitamin B6
745 synthesis. The significant induction of 4-hydroxyphenylpyruvate dioxygenase (HPDL,
746 v1g13173) in response to all four UV treatments is particularly interesting because HPDL
747 catalyzes the second reaction in the catabolism of tyrosine, an amino acid that serves as a
748 feedback inhibitor of the shikimic acid pathway in cyanobacteria (Portwich et al., 2003).
749 Furthermore, we also observed the significant induction of pyridoxine 5′-phosphate oxidase
750 (PNPO, v1g80869) and pyridoxal 5′-phosphate synthase (PdxST, v1g194582), two key
751 enzymes in the metabolism of vitamin B6, in all four UV treatments (Figure 5F). While pyridoxal
752 5′-phosphate, the active form of vitamin B6, can function as a co-enzyme in a variety of
753 enzymatic reactions, it can also be used as a Schiff base in the production of aromatic amino
754 acids in the shikimic acid pathway (Seigler, 1998). Interestingly, we also observed the
755 significant up-regulation of a transcript encoding a protein with a conserved pyridoxal-dependent

decarboxylase domain (DDC, v1g204120) found in aromatic L-amino acid decarboxylases, enzymes responsible for multiple decarboxylation reactions that convert aromatic amino acids into neuromodulators, and are also responsible for the conversion of L-3,4-dihydroxyphenylalanine (L-DOPA) and 5-hydroxytryptophan (5-HTP) into dopamine and serotonin, respectively (Ebadi and Simonneaux, 1991; Paiardini et al., 2017). However, the second to last step of the shikimic acid pathway does require a decarboxylase enzyme, so perhaps this enzyme is possibly playing a role in the production of aromatic amino acids. Further characterization of this DDC enzyme would be required to determine its phylogenetic relationship and functional role in *Nematostella*.

## 4. CONCLUSIONS

Coastal marine species experience a multitude of abiotic, biotic, and anthropogenic conditions that can exert cellular stress in complex ways when combined. While PAHs and other organic pollutants can result in severe toxicity for many species, cnidarians, like *Nematostella*, have a limited response to these substances at the organismal and the molecular level. Contrary to our prediction, *Nematostella* did not upregulate any phase I or phase II metabolic genes in response to dispersant and/or oil alone. However, when combined with ecologically relevant exposure to UV light, the toxicity of sweet crude oil and chemicals designed to minimize the environmental impact of oil spills (dispersant) leads anemones to mount an extensive molecular response as protection from cellular damage. This response included well-described components of the chemical defensome, as well as genes involved in DNA repair, and the production of UV-protective compounds and novel antioxidants. However, many questions remain regarding the activation of the “defensome” by hydrocarbon exposure in cnidarians, as well as the specific mechanisms by which they metabolize and excrete xenobiotics. Together, these results emphasize the need to consider environmental stressors in combination when determining unsafe levels in the environment and potential biomarkers to assess the health of natural populations.

## Acknowledgements

This material is based upon work supported by the National Science Foundation under Grant No. MCB1057152 (MJJ), MCB1057354 (AMT) and DEB1545539 (AMR). Any opinions, findings, and conclusions or recommendations expressed in this material are those of the authors and do not necessarily reflect the views of the National Science Foundation.

## References


Artamonova, I. I., Mushegian, A.R., 2013. Genome sequence analysis indicates that the model eukaryote *Nematostella vectensis* harbors bacterial consorts. Appl. Environ. Microbiol. 79, 6868-6873.

Balskus, E.P., Walsh, C. T., 2010. The genetic and molecular basis for sunscreen biosynthesis in cyanobacteria. Science 329, 1653-1656.

Braunshausen, A., Seebeck, F.P., 2011. Identification and characterization of the first ovothiol biosynthetic enzyme. J. Am. Chem. Soc. 133, 1757-1759.

Castellano, I., Migliaccio, O., D'Aniello, S., Merlino, A., Napolitano, A., Palumbo, A., 2016. Shedding light on ovothiol biosynthesis in marine metazoans. Sci. Rep. 6, 21506.

Chaves, I., Pokorny, R., Byrdin, M., Hoang, N., Ritz, T., Brettel, K., Essen, L.-O., van der Horst, G. T. J., Batschauer, A., Ahmad, M., 2011. The cryptochromes: blue light photoreceptors in plants and animals. Annu. Rev. Plant Biol. 62, 335-364.

Chen, Y., Kissling, G., Negishi, M., Goldstein, J.A., 2005. The nuclear receptors constitutive androstane receptor and pregnane X receptor cross-talk with hepatic nuclear factor 4alpha to synergistically activate the human CYP2C9 promoter. J. Pharmacol. Exp. Ther. 314, 1125-1133.

DeLeo, D. M., Ruiz-Ramos, D. V., Baums, I. B., Cordes, E. E., 2016. Response of deep-water corals to oil and chemical dispersant exposure. Deep Sea Res. Part II Top. Stud. Oceanogr. 129, 137-147.

Denton, G.R.W., Concepcion, L.P., Wood, H.R., Morrison, R.J., 2006. Polychlorinated biphenyls (PCBs) in marine organisms from four harbours in Guam. Mar. Poll. Bull. 52, 711-718.

Douki, T., Cadet, J., 2001. Individual determination of the yield of the main UV-induced dimeric pyrimidine photoproducts in DNA suggests a high mutagenicity of CC photolesions. *Biochemistry* 40, 2495-2501.

824 Ebadi, M., Simonneaux, V., 1991. Ambivalence on the multiplicity of mammalian aromatic L-
825 amino acid decarboxylase. Adv. Exp. Med. Biol. 294, 115-125.
826
827 Elan, R., Raam, M., Kraus, R., Brekhman, V., Sher, N., Plaschkes, I., Chalifa-Caspi, V., Lotan,
828 T., 2014. Early and late response of *Nematostella vectensis* transcriptome to heavy metals. Mol.
829 Ecol. 23, 4722-4736.
830
831 Epstein, N., Bak, R.P.M., Rinkevich, B., 2000. Toxicity of third generation dispersants and
832 dispersed Egyptian crude oil on Red Sea coral larvae. Mar. Poll. Bull. 40, 497-503.
833
834 Fawaz, M.V., Topper, M., Firestine, S. M., 2011. The ATP-grasp enzymes. Bioorg. Chem. 39,
835 185-191.
836
837 Fitzgerald, L.M., Szmant, A.M., 1997. Biosynthesis of "essential" amino acids by scleractinian
838 corals. Biochem. J. 322, 213-221.
839
840 Fleeger, J.W., Carman, K.R., Riggio, M.R., Mendelssohn, I.A., Lin, Q.X., Hou, A., Deis, D.R.,
841 Zengel, S., 2015, Recovery of salt marsh benthic microalgae and meiofauna following the
842 Deepwater Horison oil spill linked to recovery of *Spartina alterniflora*. Mar. Ecol. Prog. Ser., 536,
843 39-54.
844
845 Fritsche, E., Schafer, C., Calles, C., Bernsmann, T., Bernshausen, T., Wurm, M., Hubenthal, U.,
846 Cline, J.E., Hajimiragha, H., Schroeder, P., Klotz, L.O., Rannug, A., Furst, P., Hanenberg, H.,
847 Abel, J., Krutmann, J., 2007. Lighening up the UV response by identification of the
848 arylhydrocarbon receptor as a cytoplasmic target for ultraviolet B radiation. Proc. Natl. Acad.
849 Sci. U.S.A. 104, 8851-8856.
850
851 Garcia, T.I., Shen, Y., Crawford, D., Oleksiak, M. F., Whitehead, A., Walter, R. B., 2012. RNA-
852 seq reveals complex genetic response to deepwater horizon oil release in *Fundulus grandis.*
853 BMC Genomics 13, 474
854
855 Gassman, N.J., Kennedy, C.J., 1992. Cytochrome P-450 content and xenobiotic metabolizing
856 enzyme activities in the scleractinan coral, *Favia fragum* (Esper). Bull. Mar. Sci. 50, 320-330.
857

858 Goldstone, J.V., Hamdoun, A., Cole, B.J., Howard-Ashby, M., Nebert, D.W., Scally, M.,
859 Dean, M., Epel, D., Hahn, M.E., Stegeman, J.J., 2006. The chemical defensome:
860 environmental sensing and response genes in the *Strongylocentrotus purpuratus*
861 genome. Dev. Biol. 300, 366-384.
862
863 Goldstone, J.V., 2008. Environmental sensing and response genes in cnidarian: the chemical
864 defensome in the sea anemone *Nematostella vectensis*. Cell Biol. Toxicol. 24, 483-502.
865
866 Goodbody-Gringley, G., Wetzel, D. L., Gillon, D., Pulster, E., Miller, A., Ritchie, K. B., 2013.
867 Toxicity of Deepwater Horizon source oil and the chemical dispersant, Corexit 9500, to coral
868 larvae. PLoS One 8, e45574/
869
870 Goncharenko, K.V., Vit, A., Blankenfeldt, W., Seebeck, F. P., 2015. Structure of the sulfoxide
871 synthase EgtB from the ergothioneine biosynthetic pathway. Angew. Chem. Int. Ed. 54, 2821-
872 2824.
873
874 Grzanka, D., Domaniewski, J., Grzanka, A., Zuryn, A., 2006. Ultraviolet radiation (UV) induces
875 reorganization of actin cytoskeleton in CHOAA8 cells. Neoplasma 53, 328-332.
876
877 Hahn, M. E., Karchner, S. I., Merson, R. R., 2017. Diversity as opportunity: insights from 600
878 million years of AHR evolution. Curr. Opin. Toxicol. 2, 58-71.
879
880 Hamdan, L.J., Fulmer, P.A., 2011. Effects of Corexit EC9500A on bacteria from a beach oiled
881 by the Deepwater Horizon spill. Aquat. Microb. Ecol. 63, 101-109.
882
883 Hannam M.L., Bamber S.D., Galloway T.S., Moody A.J., Jones M.B., 2010. Effects of the model
884 PAH phenanthrene on immune function and oxidative stress in the haemolymph of the
885 temperate scallop *Pecten maximus*. Chemosphere 78, 779-784.
886
887 Heffernan, L. M., Winston, G. W., 1998. Spectral analysis and catalytic activities of the
888 microsomal mixed-function oxidase system of the sea anemone (phylum Cnidaria). Comp.
889 Biochem. Physiol. C Pharmacol. Toxicol. Endocrinol. 121, 371-383.
890

Heffernan, L. M., Winston, G. W., 2000. Distribution of microsomal CO-binding chromophores and EROD activity in sea anemone tissues. Mar. Environ. Res. 50, 23-27.

Helm, R. R., Siebert, S., Tulin, S., Smith, J., Dunn, C. W., 2013. Characterization of differential transcript abundance through time during *Nematostella vectensis* development. BMC Genomics 14, 266.

Hu, Z., Jin, S., Scotto, K.W., 2000. Transcriptional activation of the MDR1 gene by UV radiation Role of NF-Y and Sp1. J. Biol. Chem. 275, 2979-2985.

Hylland, K., 2006. Polycyclic aromatic hydrocarbon (PAH) ecotoxicology in marine ecosystems. J. Toxicol. Environ, Health A 69, 109-123.

Jenny, M.J., Walton, W.C., Payton, S.L., Powers, J.M., Findlay, R.H., O'Shields, B, Diggins, K., Pinkerton, M., Porter, D., Crane, D.M., Tapley, J., Cunningham, C., 2016. Transcriptomic evaluation of the American oyster, *Crassostrea virginica*, deployed during the Deepwater Horizon oil spill: Evidence of an active hydrocarbon response pathway. Mar. Environ. Res. 120, 166-181.

Jover, R., Moya, M., Gómez-Lechón, M.J., 2009. Transcriptional regulation of cytochrome p450 genes by the nuclear receptor hepatocyte nuclear factor 4-alpha. Curr. Drug Metab. 10, 508-519.

Kennedy, C., Gassman, N., Walsh, P., 1992. The fate of benzo[a]pyrene in the scleractinian corals *Favia fragum* and *Montastrea annularis*. Mar. Biol. 113, 313-318.

Leite, J.C., de Vasconcelos, R.B., da Silva, S.G., de Sigueira-Junior, J.P., Marques-Santos, L.F., 2014. ATP-binding cassette transporters protect sea urchin gametes and embryonic cells against the harmful effects of ultraviolet light. Mol. Reprod. Dev. 81, 66-83.

Lin, X., Cerenius, L., Lee, B.L., Soderhall, K., 2007. Purification of properoxinectin, a myeloperoxidase homologue and its activation to a cell adhesion molecule. Biochim. Biophys. Acta. 1770, 87-93.

925 Lin, Q., Mendelssohn, I.A., 2012. Impacts and recovery of the Deepwater Horizon oil spill on
926 vegetation structure and function of coastal salt marshes in the northern Gulf of Mexico.
927 Environ. Sci. Technol. 46, 3737-3743.
928
929 Liu, N., Pan, L., Miao, J., Xu, C., Zhang, L., 2010. Molecular cloning and sequence
930 analysis and the response of a aryl hydrocarbon receptor homologue gene in
931 the clam *Ruditapes philippinarum* exposed to benzo(a)pyrene. Comp. Biochem.
932 Physiol. Part C Toxicol. Pharmacol. 152, 279-287.
933
934 Maekawa, T.L., Takahashi, T.A., Fujihara, M., Akasaka, J., Fujkawa, S., Minami, M., Sekiquchi,
935 S., 1996. Effects of ultraviolet B irradiation on cell-cell interation; implication of morphological
936 changes and actin filaments in irradiated cell. Clin. Exp. Immunol. 105, 389-396.
937
938 Masaki, H., Sakurai, H., 1997. Increased generation of hydrogen peroxide possibly from
939 mitochondrial respiratory chain after UVB irradiation of murine fibroblasts. J. Dermatol. Sci. 14,
940 207-216.
941
942 Mashabela, G.T.M., Seebeck, F. P., 2013. Substrate specificity of an oxygen dependent
943 sulfoxide synthase in ovothiol biosynthesis. Chem. Commun. 49, 7714-7716.
944
945 Matsunaga, T., Hieda, K., Nikaido, O., 1991. Wavelength dependent formation of thymine
946 dimers and (6-4)photoproducts in DNA by monochromatic ultraviolet light ranging from 150 to
947 365 nm. Photochem. Photobiol. 54, 403-410.
948
949 McCall, B.D., Pennings, S.C., 2012. Disturbance and recovery of salt marsh arthropod
950 communities following BP Deepwater Horizon oil spill. PLoS One 7, e32735.
951
952 Natter, M., Keevan, J., Wang, Y., Keimowitz, A. R., Okeke, B. C., Son, A., Lee, M. K., 2012.
953 Level and degradation of Deepwater Horizon spilled oil in coastal marsh sediments and pore-
954 water. Environ. Sci. Technol. 46, 5744-5755.
955
956 Neff, J.M., 2002. Bioaccumulation in Marine Organisms: Effects of Contaminants from Oil Well-
957 produced Water. Amsterdam: Elsevier Science.
958

959 Negri, A.P., Heyward, A.J., 2000. Inhibition of fertilization and larval metamorphosis of the coral
960 Acropora millepora (Ehrenberg, 1834) by petroleum products. Mar. Poll. Bull. *41*, 420-427.
961
962 Niggli, H.J., Cerutti, P. A., 1983. Cyclobutane-type pyrimidine formation and excision in human
963 skin fibroblasts after irradiation with 313 nm ultraviolet light. Biochemistry 22, 1390-1395.
964
965 Oren A., Gunde-Cimerman N., 2007. Mycosporines and mycosporine-like amino acids: UV
966 protectants or multipurpose secondary metabolites? FEMS Microbiol. Lett. 269, 1-10.
967
968 Oren, M., Tarrant, A. M., Alon, S., Simon-Blecher, N., Elbaz, I., Appelbaum, L., Levy, O., 2015.
969 Profiling molecular and behavioral circadian rhythms in the non-symbiotic sea anemone
970 *Nematostella vectensis.* Sci. Rep. 5, 11418.
971
972 Paiardini A., Giardina, G., Rossignoli, G., Voltattorni, C. B., Bertoldi, M., 2017. New insights
973 emerging from recent investigations on human group II pyridoxal 5'-phosphate decarboxylases.
974 Curr. Med. Chem. 24, 226-244.
975
976 Papageorgiou, A.P., Heymans, S., 2014. Peroxidasin-like protein: expanding the horizons or
977 matrix biology. Cardiovasc. Res. 101, 342-343.
978
979 Paul, B. D., Snyder, S. H., 2010. The unusual amino acid L-ergothioneine is a physiologic
980 cytoprotectant. Cell Death Differ. 17, 1134-1140.
981
982 Peters, E.C., Gassman, N.J., Firman, J.C., Richmond, R.H., Power, E.A., 1997. Ecotoxicology
983 of tropical marine ecosystems. Environ. Toxicol. Chem. 16, 12-40.
984
985 Pfeifer, G.P, Young-Hyun, Y., Besaratinia, A., 2005. Mutations induced by ultraviolet light.
986 Mutat. Res. 571, 19-31.
987
988 Pilcher, W., Miles, S., Tang, S., Mayer, G., Whitehead, A., 2014. Genomic and genotoxic
989 responses to controlled weathered-oil exposures confirm and extend field studies on impacts of
990 the Deepwater Horizon oil spill on native killifish. PLoS One 9, e106351.
991

992 Portwich, A., Garcia-Pichel, F., 2003. Biosynthetic pathway of mycosporines (mycosporine-like
993 amino acids) in the cyanobacterium *Chlorogloeopsis* sp. strain PCC 6912. Phycologia 42, 384-
994 392.
995
996 Puthumana, J., Lee, M.-C., Park, J.C., Kim, H.-S., Hwang, D.-S., Han, J., Lee, J.-S., 2017.
997 Ultraviolet B radiation induces impaired lifecycle traits and modulates expression of cytochrome
998 P450 (CYP) genes in the copepod *Tigriopus japonicus*.
999 Rahman, M. A., Sinha, S., Sachan, S., Kumar, G., Singh, S. K., Sundaram, S., 2014. Analysis
1000 of proteins involved in the production of MAAs in two cyanobacteria *Synechocystis* PCC 6803
1001 and Anabaena cylindrical. Bioinformation 10, 449-453.
1002
1003 Ramseur, J.L., 2010. Deepwater Horizon oil spill: the fate of the oil. Washington, DC:
1004 Congressional Research Service, Library of Congress. https://fas.org/sgp/crs/misc/R41531.pdf
1005
1006 Reitzel A.M., Chu T., Edquist S., Genovese C., Church C., Tarrant A.M., Finnerty J.R., 2013.
1007 Physiological and developmental responses to temperature by the sea anemone *Nematostella*
1008 *vectensis*. Mar. Ecol. Prog. Ser. 484, 115-130.
1009
1010 Reitzel, A.M., Passamaneck, Y.J., Karchner, S.I., Franks, D.G., Martindale, M.Q., Tarrant, A.M.,
1011 Hahn, M.E., 2014. Aryl hydrocarbon receptor (AHR) in the cnidarian *Nematostella vectensis*:
1012 comparative expression, protein interactions, and ligand binding. Dev. Genes Ecol. 224, 13-24.
1013
1014 Reitzel, A.M., Sullivan, J.C., Traylor-Knowles, N., Finnerty, J.R., 2008. Genomic survey of
1015 candidate stress-response genes in the estuarine anemone *Nematostella vectensis*. Biol. Bull.
1016 214, 233-254.
1017
1018 Reitzel, A., Tarrant, A., 2009. Nuclear receptor complement of the cnidarian *Nematostella*
1019 *vectensis*: phylogenetic relationships and developmental expression patterns. BMC Evol. Biol.
1020 9, 230.
1021
1022 Robinson M. D., McCarthy D. J., Smyth G. K., 2009. edgeR: a Bioconductor package for
1023 differential expression analysis of digital gene expression data. Bioinformatics 26:139–140.
1024

Rozas L.P., Minello T.J., Miles M.S., 2014. Effect of Deepwater Horizon oil on growth rates of juvenile penaeid shrimps. Estuar. Coast. 37, 1403-1414.

Rougée, L., Downs, C.A., Richmond, R.H., Ostrander, G. K., 2006. Alteration of normal cellular profiles in the scleractinian coral (*Pocillopora damicornis*) following laboratory exposure to fuel oil. Environ. Toxicol. Chem. 25, 3181-3187.

Sancar, A., 2003. Structure and function of DNA photolyase and cryptochrome blue-light photoreceptors. Chem. Rev. 103, 2203-2237.

Schlezinger, J.J., Struntz, W.D., Goldstone, J.V., Stegeman, J.J., 2006. Uncoupling of cytochrome P450 1A and stimulation of reactive oxygen species production by co-planar polychlorinated biphenyl congeners. Aquat. Toxicol. 77, 422-432.

Schlezinger, J.J., White, R.D., Stegeman, J.J., 1999. Oxidative inactivation of cytochrome P-450 1A (CYP1A) stimulated by 3,3',4,4'-tetrachlorobiphenyl: production of reactive oxygen by vertebrate CYP1As. Mol. Pharmacol. 56, 588-597.

Seigler, D. S., 1998. Plant Secondary Metabolism. Springer US.

Sesto, A., Navarro, M., Burslem, F., Jorcano, J.L., 2002. Analysis of the ultraviolet B response in primary human keratinocytes using oligonucleotide microarrays. Proc. Natl. Acad. Sci. U.S.A. 99, 2965-2970.

Shafirovich, V., Kropachev, K., Anderson, T., Liu, Z., Kolbanovskiy, M., Martin, B.D., Sugden, K., Shim, Y., Chen, X., Min, J.H., Geacintov, N. E., 2016. Base and nucleotide excision repair of oxidatively generated guanine lesions in DNA. J. Biol. Chem. 291, 5309-5319.

Shah, P., He, Y. Y., 2015. Molecular regulation of UV-induced DNA repair. Photochem. Photobiol. 91, 254-264.

Shapiro, B.M., Turner, E., 1988. Oxidative stress and the role of novel thiol compounds at fertilization. Biofactors 1, 85-88.

Shick J.M., Dunlap W.C., 2002. Mycosporine-like amino acids and related gadusols: biosynthesis, accumulation, and UV-protective functions in aquatic organisms. Ann. Rev. Physiol. 64, 223-262.

Shick. J. M., Dunlap, W. C., Pearse, J. S., Pearse, V. B., 2002. Mycosporine-like amino acid content in four species of sea anemones in the genus *Anthopleura* reflects phylogenetic but not environmental or symbiotic relationship. Biol. Bull. 203, 315-330.

Shinzato, C., Shoquchi, E., Kawashima, T., Hamada, M., Hisata, K., Tanaka, M., Fujie, M., Fujiwara, M., Koyanagi, R., Ikuta, T., Fujiyama, A., Miller, D. J., Satoh, N., 2011. Using the *Acropora digitifera* genome to understand coral responses to environmental change. Nature 476, 320-323.

Shoguchi, E., Tanaka, M., Shinzato, C., Kawashima, T., Satoh, N., 2013. A genome-wide survey of photoreceptor and circadian genes in the coral, *Acropora digitifera*. Gene 515, 426-431.

Solbakken, J., Knap, A., Sleeter, T., Searle, C., Palmork, K., 1984. Investigation into the fate of $^{14}$C-labeled xenobiotics (naphthalene, phenanthrene, 2,4,5,2',2',5'-hexachlorobiphenyl, octachlorostyrene) in Bermudian corals. Mar. Ecol. Prog. Ser. 16, 149-154.

Song, H., Leninger, M., Lee, N., Liu. P., 2013. Regioselectivity of the oxidative C-S bond formation in ergothioneine and ovothiol biosynthesis. Org. Lett. 15, 4854-4857.

Starcevic, A., Akthar, S., Dunlap, W. C., Shick, J. M., Hranueli, D., Cullum, J., Long, P. F., 2008. Enzymes of the shikimic acid pathway encoded in the genome of a basal metazoan, *Nematostella vectensis*, have microbial origins. Proc. Natl. Acad. Sci.U.S.A. 105, 2533-2537.

Stefanik D.J., Friedman L.E., Finnerty J.R., 2013. Collecting, rearing, spawning and inducing regeneration of the starlet sea anemone, *Nematostella vectensis*. Nat. Protoc. 8, 916-923.

Stout, S. A., Payne, J. R., Emsbo-Mattingly, S. D., Baker, G., 2016. Weathering of field-collected floating and stranded Macondo oils during and shortly after the Deepwater Horizon oil spill. Mar. Poll. Bull. 105, 7-22.

Tarrant, A. M., Gilmore, T. D., Reitzel, A. M., Levy, O., Technau, U., Martindale, M. Q., 2015. Current directions and future perspectives from the third *Nematostella* research conference. Zoology 118, 135-140.

Tarrant, A. M., Reitzel, A. M., Kwok, C. K., Jenny, M. J., 2014. Activation of the cnidarian oxidative stress response by ultraviolet radiation, polycyclic aromatic hydrocarbons and crude oil. J. Exp. Biol. 217, 1444-1453.

Tirona, R.G., Lee, W., Leake. B.F., Lan, L.B., Cline, C.B., Lamba, V., Parviz, F., Duncan, S.A., Inoue, Y., Gonzalez, F.J., Schuetz, E.G., Kim, R.B., 2003. The orphan nuclear receptor HNF4alpha determines PXR- and CAR-mediated xenobiotic induction of CYP3A4. Nat. Med. 9, 220-224.

Turner, E., Klevit, R., Hopkins, P. B., and Shapiro, B. M., 1986. Ovothiol: a novel thiohistidine compound from sea urchin eggs that confers NAD(P)H-O2 oxidoreductase activity on ovoperoxidase. J. Biol. Chem. 261, 13056-13063.

Turner, E., Klevit, R., Hager, L. J., Shapiro, B. M., 1987. Ovothiols, a family of redox-active mercaptohistidine compounds from marine invertebrate eggs. Biochemistry 26, 4028-4036.

Tsai, M.-L., Chang, K.-Y., Chiang, C.-S., Shu, W.-Y, Weng, T.-C., Chen, C.R., Huang, C.-L., Lin, H.-K., Hsu, I.C., 2009. UVB radiation induces persistent activation of ribosome and oxidative phosphorylation pathways. Radiat. Res. 171, 716-724.

Uchiumi, T., Kohno, K., Tanimura, H., Matsuo, K., Sato, S., Uchida, Y., Kuwano, M., 1993. Enhanced expression of the human multidruo resistance 1 gene in response to UV light irradiation. Cell Growth Differ. 4, 147-157.

van Dam J.W., Negri A.P., Uthicke S., Mueller J.F., 2011. Chemical pollution on coral reefs: exposure and ecological effects, in: Sánchez-Bayo, S., van den Brink, P.J., Mann, R.M. (Eds.), Ecological impacts of toxic chemicals. Bentham Science Publishers, pp.187-211

Venn, A.A., Quinn, J., Jones, R., Bodnar, A., 2009. P-glycoprotein (multi-xenobiotic resistance) and heat shock protein gene expression in the reef coral *Montastraea franksi* in response to environmental toxicants. Aquat. Toxicol. 93, 188-195.

Wakabayashi, N., Slocum, S.L., Skoko, J.J., Shin, S., Kensler, T.W., 2010. When NRF2 talks, who's listening? Antioxid Redox Signal., 13, 1649-1663.

Wei, Y.D., Helleberg, H., Rannug, U., Rannug, A., 1998. Rapid and transient induction of CYP1A1 gene expression in human cells by the tryptophan photoproduct 6-formylindolo[3,2-b]carbazole. Chem. Biol. Interact. 110, 39-55.

Wei, Y.D., Rannug, U., Rannug, A., 1999. UV-induced CYP1A1 gene expression in human cells is mediated by tryptophan. Chem. Biol. Interact. 118, 127-140.

Xu, E.G., Mager, E. M., Grosell, M., Pasparakis, C., Schlenker, L. S., Stieglitz, J. D., Benetti, D., Hazard, E. S., Courtney, S. M., Diamante, G., Freitas, J., Hardiman, G., Schlenk, D., 2016. Time- and oil-dependent transcriptomic and physiological responses to Deepwater Horizon oil in Mahi-Mahi (*Coryphaena hippurus*) embryos and larvae. Environ. Sci. Technol. 50, 7842-7851.

Young, M. D., Wakefield, M. J., Smyth, G. K., Oshlack, A., 2010. Gene ontology analysis for RNA-seq: accounting for selection bias. Genome Biol. 11, R14.

Zengel, S., Montague, C.L., Pennings, S.C., Powers, S.P., Steinhoff, M., Fricano, G., Schlemme, C., Zhang, M., Oehrig, J., Nixon, Z., Rouhani, S., 2016. Impacts of the Deepwater Horizon oil spill on salt marsh periwinkles (*Littoraria irrorata*). Environ. Sci. Technol. 50, 643-652.

Zhu, L., Qu, K., Xia, B., Sun, X., Chen, B., 2016. Transcriptomic response to water accommodated fraction of crude oil exposure in the gill of Japanese flounder, *Paralichthys olivaceus*. Mar. Poll. Bull. 106, 283-291.

- Crude oil exposure elicits a modest transcriptomic change in *Nematostella*.
- Dispersant produces a stronger transcriptomic response compared to crude oil.
- UV radiation exposure produces dramatic changes in global gene expression.
- UV exposure synergizes crude oil and dispersant toxicity in *Nematostella*.
- Data suggest that *Nematostella* is capable of *de novo* MAA synthesis.